Legendre polynomial modeling of composite bulk acoustic wave resonators

A. Raherison, F.E. Ratolojanahary, Jean-Etienne Lefebvre, L. Elmaimouni

Legendre polynomial modeling of composite bulk acoustic wave resonators

Cite as: J. Appl. Phys. **104**, 014508 (2008); https://doi.org/10.1063/1.2953096
Submitted: 13 February 2008 • Accepted: 06 May 2008 • Published Online: 11 July 2008

A. Raherison, F. E. Ratolojanahary, J. E. Lefebvre, et al.

Legendre polynomial modeling of composite bulk acoustic wave resonators

A. Raherison,[1] F. E. Ratolojanahary,[1] J. E. Lefebvre,[2,a)] and L. Elmaimouni[3]
[1]*LAPAUF, Université de Fianarantsoa, 301 Fianarantsoa, Madagascar*
[2]*IEMN-DOAE, Université du Mont Houy, 59313 Valenciennes Cedex 9, France*
[3]*Faculté polydisciplinaire d'Ouarzazate, Université Ibn Zohr, 45000 Ouarzazate, Morocco*

(Received 13 February 2008; accepted 6 May 2008; published online 11 July 2008)

The Legendre polynomial method has been extended to the modeling of bulk acoustic wave (BAW) resonators. Modifications have been made to the formulation in order to account for large differences in the physical properties of adjoining layers and to take into account the electric source. A unique formalism has been obtained which allows for both harmonic and modal analyses. Resonance and antiresonance frequencies, electric input impedance, electromechanical coupling coefficients, and quality factors have been obtained for an aluminum/zinc oxide/aluminum (Al/ZnO/Al) BAW resonator. The results are in excellent agreement with analytical results. © *2008 American Institute of Physics*. [DOI: 10.1063/1.2953096]

I. INTRODUCTION

The challenge of ultraminiaturization and monolithic integration of resonators and radio frequency (rf) filters as core components in communication systems is becoming more intense. The tremendous growth in wireless and mobile communication systems has led to a widespread demand for filters in the range of 1–10 GHz.[1] Conventional surface acoustic wave (SAW) technology has its limits and cannot meet the required specifications in this frequency range. Bulk acoustic wave (BAW) resonators based microwave filters have the advantage of being smaller, and of lower cost when mass produced and are compatible with semiconductor processes in this frequency range. They are investigated in order to develop the required high-performance components.[2] Design and optimization of BAW resonators call for efficient simulation tools.

The polynomial method provides excellent precision for the waveguides studied for both planar and cylindrical multilayered structures.[3–6] The method uses constitutive and propagation equations to describe the structure; it is easy to implement for numerical calculations, with remarkable simplicity when using physical quantities such as elastic stiffness, permittivity, and density through which the boundary conditions are automatically incorporated. Moreover, the acoustic field distributions are easily obtained.[3–6] However, (i) it has only been applied to propagating waves and never for analyzing a structure with standing waves, as required for the study of BAW resonators; (ii) its convergence depends on the properties of the materials, i.e., good convergence for structures constituted of layers of materials with parameters close to each other and poor convergence if they are dissimilar; (iii) it has been applied without any source term.[5]

BAW resonators consist of a piezolayer sandwiched between two metal electrodes. Therefore, the parameters of the constituent layers are dissimilar in nature. The calculation of the electric input impedance of the resonator requires an electrical excitation, either voltage or current. Furthermore, these devices are based on standing waves. Thus, an extension of the polynomial method is needed for modeling BAW resonators. In Sec. II, the mathematical formulation is presented in detail. The problem linked to the method's convergence due to structures composed of dissimilar layers was solved by an anticipation process. The introduction of excitation sources is illustrated. In Sec. III, this method was implemented in a numerical simulation. This approach was validated by studying an Al/ZnO/Al structure; the results were compared to the results obtained using an analytical model. The approach proposed provides a unique formalism to describe both harmonic and modal analyses. A summary is given in Sec. IV.

II. MATHEMATICAL FORMULATION

A. Structure

The structure studied is a ZnO layer sandwiched between two thick aluminum electrodes, polarized by an electrical source, either voltage or current, as shown in Fig. 1. It is assumed that the metal electrodes are perfect conductors. The bottom electrode is grounded. Throughout this paper, $\exp(i\omega t)$ time dependence is assumed.

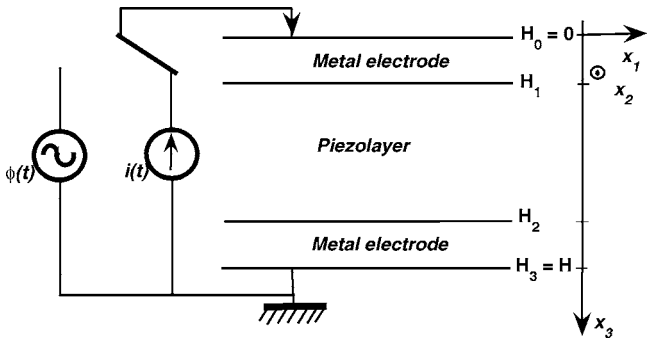

FIG. 1. Schematic diagram of a composite BAW resonator.

a)Author to whom correspondence should be addressed. Electronic mail: jean-etienne.lefebvre@univ-valenciennes.fr.

Each medium is characterized by its stiffness tensor c, piezoelectric tensor e, permittivity tensor ε, and density ρ. The coordinate axes x_1, x_2, and x_3 coincide with the crystal axes X, Y, and Z and the x_3 is normal to the layer interfaces.

B. Constitutive equations

ZnO is a piezoelectric material within which an electromechanical coupling phenomenon occurs. This phenomenon is defined by the constitutive equations[7]

$$T_{ac} = c^D_{acbd}\frac{\partial u_b}{\partial x_d} - h_{dac}D_d, \tag{1a}$$

$$\frac{\partial \phi}{\partial x_c} = h_{cbd}\frac{\partial u_b}{\partial x_d} - \beta_{cd}D_d, \tag{1b}$$

with

$$\beta_{cd} = \varepsilon^{-1}_{cd},$$

$$c^D_{acbd} = c^E_{acbd} + e_{fac}\beta_{fk}e_{kbd},$$

$$h_{cbd} = e_{abd}\beta_{ac},$$

where u_b represents the components of particle displacement, T_{ac} and D_c are the stress and electric displacement, and ϕ is the electric potential. The subscripts a, b, c, d, f, and k take on the values 1, 2, and 3 and summation over repeated indices is implied throughout this paper, unless otherwise specified. Aluminum is assumed to be a perfect conductor. Thus, Eqs. (1a) and (1b) become

$$T_{ac} = c^E_{acbd}\frac{\partial u_b}{\partial x_d}, \tag{2a}$$

$$\frac{\partial \phi}{\partial x_c} = 0. \tag{2b}$$

The structure is assumed to be laterally unlimited with no variations in the lateral x_1 and x_2 directions. It is also assumed that a uniform bulk acoustic longitudinal wave propagates along the x_3 direction. So $\partial/\partial x_1 = \partial/\partial x_2 = 0$ and the nonzero field components are T_{33} and D_3. Hence, the constitutive relations can be rewritten as

$$T = c^D\frac{\partial u}{\partial x} - hD, \tag{3a}$$

$$\frac{\partial \phi}{\partial x} = h\frac{\partial u}{\partial x} - \beta D, \tag{3b}$$

where the subscripts have been dropped for convenience: $T = T_{33}$, $D = D_3$, $u = u_3$, $e = e_{333}$, $x = x_3$, $\varepsilon = \varepsilon_{33}$, $\beta = \varepsilon^{-1}_{33}$, $c^D = c^E_{3333} + e^2_{333}\beta$, and $h = e_{333}\beta$. For the electrodes, $h = \beta = 0$.

C. Propagation equations

The field equations governing wave propagation in the structure can be written as

$$\frac{\partial T}{\partial x} = -\rho^S\omega^2 u, \tag{4a}$$

$$\frac{\partial D}{\partial x} = 0, \tag{4b}$$

where the superscript s denotes the global structure.

The boundary conditions require that (i) the normal stress should be zero at the two mechanically free terminal surfaces; (ii) the normal stress, the electric potential, and the particle displacement should be continuous at the interfaces. Furthermore, the normal electric displacement is assumed to be zero outside the resonator.

The spatial coordinate is transformed to be dimensionless $q = x/\mathrm{H}$; H is the resonator thickness.

D. Resolution method: Anticipation of slope discontinuities

In previous studies,[3–6] the particle displacement components were expanded in terms of a set of polynomials which is complete and orthonormal over the entire interval of interest:

$$u_L(q) = p_m Q_m(q), \quad 0 \leqslant q \leqslant 1, \tag{5a}$$

where p_m is the expansion coefficient and $Q_m(q) = \sqrt{2m+1}P_m(2q-1)$, where P_m represents the mth Legendre polynomial.

In a previous paper,[5] the authors pointed out that the problem could only be solved if the parameters of the constituent layers are close to each other. For layers of materials that are very dissimilar in nature, as the Legendre polynomials and their derivatives are continuous on the interval of interest, it was shown that, to fit the field profiles which are discontinuous either in value or in slope at the interfaces, an important number of expansion terms are required and convergence is either poor or impossible depending on the dissimilarity level. To circumvent this difficulty, we propose incorporating slope discontinuities directly into the field representations by choosing, for the mechanical displacement, a specific expression within each layer rather than a unique expression (5a) over the whole range of interest as it has been done up to now.

From now on, indices 1, 2, and 3 refer, respectively, to the top electrode, the piezolayer, and the bottom electrode. In the piezolayer, numbered 2, for mechanical displacement, the usual expansion has been kept:

$$u_2(q) = u_L(q), \quad \frac{H_1}{H} < q < \frac{H_2}{H}. \tag{5b}$$

According to Eq. (4b), the electrical displacement D is a constant that is hereby denoted by D_0. For mechanical displacements u_1 and u_3, in the top and bottom electrodes, respectively, an expression deduced from the continuity of both the mechanical displacement and the normal stress at the interfaces, but also from the stress slope discontinuity at these same interfaces, has been adopted.

In what follows, the "classic method" is a method with a unique polynomial expression over the entire interval of interest and the "anticipation method" is a method with a specific polynomial expression for each layer.

It is shown in Appendix A that the following expression meets the above requirements:

$$u_i(q) = \frac{\rho_i}{\rho_2}\frac{c_2^D}{c_i}u_L(q) + \frac{c_2^D}{c_i}\left(1-\frac{\rho_i}{\rho_2}\right)(q-q_i)\left.\frac{\partial u_L}{\partial q}\right|_{q=q_i} + \left(1-\frac{\rho_i}{\rho_2}\frac{c_2^D}{c_i}\right)u_L(q_i) - \frac{\mathrm{H}h_2}{c_i}(q-q_i)D_0, \quad i=1,3, \tag{5c}$$

with no summation over the indices i. $c_i = c_i^D = c_i^E$ for the electrodes; $q_1 = \mathrm{H}_1/\mathrm{H}$ and $q_3 = \mathrm{H}_2/\mathrm{H}$.

In order (i) to describe the fields in the whole structure and (ii) to automatically incorporate the boundary conditions on the outer surfaces,[3] the rectangular window function π_i is introduced and is defined as

$$\pi_i(q) = \begin{cases} 1 & \text{if } \dfrac{\mathrm{H}_{i-1}}{\mathrm{H}} \leqslant q \leqslant \dfrac{\mathrm{H}_i}{\mathrm{H}} \\ 0 & \text{otherwise} \end{cases} \qquad \text{with } i=1,2,3. \tag{6}$$

Thus, the effective density and the field variables within the structure can be written as

$$\rho^S = \rho_i \pi_i(q), \quad i=1,2,3, \tag{7a}$$

$$u(q) = u_i(q)\pi_i(q), \quad i=1,2,3, \tag{7b}$$

$$D(q) = D_2(q)\pi_2(q), \tag{7c}$$

$$T(q) = \left(\frac{c_1}{\mathrm{H}}\frac{\partial u_1}{\partial q}\right)\pi_1(q) + \left(\frac{c_2^D}{\mathrm{H}}\frac{\partial u_2}{\partial q} - h_2 D_2(q)\right)\pi_2(q) + \left(\frac{c_3}{\mathrm{H}}\frac{\partial u_3}{\partial q}\right)\pi_3(q). \tag{7d}$$

Substituting Eq. (7d) into Eq. (4a), we have

$$\begin{aligned} c_2^D\left(\frac{\rho_i}{\rho_2}\frac{\partial}{\partial q}\left[\pi_i(q)\frac{\partial u_L}{\partial q}\right] + \frac{\partial}{\partial q}\left[\pi_2(q)\frac{\partial u_L}{\partial q}\right] + \left(1-\frac{\rho_i}{\rho_2}\right)\frac{\partial \pi_i}{\partial q}\left.\frac{\partial u_L}{\partial q}\right|_{q=q_i}\right) - \mathrm{H}h_2\frac{\partial \Pi(q)}{\partial q}D_0 \\ = -(\omega\mathrm{H})^2\left\{\left(\frac{\rho_i^2}{\rho_2}\frac{c_2^D}{c_i}\pi_i(q) + \rho_2\pi_2(q)\right)u_L(q) + \frac{\rho_i c_2^D}{c_i}\left(1-\frac{\rho_i}{\rho_2}\right)(q-q_i)\pi_i(q)\left.\frac{\partial u_L}{\partial q}\right|_{q=q_i} + \rho_i\pi_i(q)\left(1-\frac{\rho_i}{\rho_2}\frac{c_2^D}{c_i}\right)u_L(q_i)\right\} \\ + (\omega\mathrm{H})^2\frac{\rho_i \mathrm{H}h_2}{c_i}(q-q_i)\pi_i(q)D_0, \quad i=1,3, \end{aligned} \tag{8}$$

where $\Pi(q) = \pi_1(q) + \pi_2(q) + \pi_3(q)$.

Substituting the particle displacement u_L equation (5a) into Eq. (8) and by using the orthonormal property of Q_m polynomials, we finally obtain an infinite system of linear equations with p_m as an unknown and ωH as a parameter:

$$\frac{c_2^D}{\rho_2}[AA1_{jm} + (\omega\mathrm{H})^2 BB1_{jm}]p_m = \mathrm{H}h_2\{[Q_j^*(0) - Q_j^*(1)] + (\omega\mathrm{H})^2 CC_j\}D_0, \tag{9}$$

where $AA1_{jm}$, $BB1_{jm}$, and CC_j are infinite square matrices evaluated in Appendix B.

E. Analytical solutions

The developed model allows both harmonic and modal analyses to be performed. The use of either voltage or current as sources of excitation gives direct access to the resonance and the antiresonance frequencies, respectively.

According to Ampère's law, the displacement current density in the piezolayer is

$$J(q,t) = \frac{\partial D_2}{\partial t} = i\omega D_0 e^{i\omega t} \quad \text{where } i = \sqrt{-1}, \tag{10a}$$

and the electrical current I that flows through the electrode of area S is given by

$$I = JS = i\omega D_0 S. \tag{10b}$$

Integrating Eq. (3b) over q from q_1 to q_3 gives the voltage U applied between the electrodes of the structure:

$$U = h_2[u_2(q_1) - u_2(q_3)] - \beta_2(\mathrm{H}_1 - \mathrm{H}_2)D_0. \tag{11}$$

1. Harmonic analysis: Current excitation method

In this excitation mode, the unknown p_m is written in terms of the imposed electrical current I. Substituting the electric displacement D_0 equation (10b) into Eq. (9) gives

$$\frac{c_2^D}{\rho_2}[AA1_{jm} + (\omega\mathrm{H})^2 BB1_{jm}]p_m = \frac{\mathrm{H}h_2}{i\omega S}\{[Q_j^*(0) - Q_j^*(I)] + (\omega\mathrm{H})^2 CC_j\}I, \tag{12a}$$

where I is an arbitrary value. Dividing Eq. (11) by Eq. (10b) and replacing the particle displacement u_L by its expression (5a) gives the electric input impedance

$$Z_{\mathrm{in}} = \frac{U}{I} = \frac{\mathrm{H}h_2^2\rho_2}{i\omega S c_2^D}[Q_m(q_1) - Q_m(q_3)](AA1_{jm} + (\omega\mathrm{H})^2 BB1_{jm})^{-1} \times\{Q_j^*(0) - Q_j^*(1) + (\omega\mathrm{H})^2 CC_j\} - \beta_2\frac{\mathrm{H}_1 - \mathrm{H}_2}{i\omega S}. \tag{12b}$$

2. Harmonic analysis: Voltage excitation method

In this excitation mode, the unknown p_m is written in terms of the imposed electrical potential U. Substituting the electric displacement D_0 obtained from Eq. (11) into Eq. (9), we have

$$\left[\frac{c_2^D}{\rho_2}(AA1_{jm}+(\omega \mathrm{H})^2 BB1_{jm}) + \frac{\mathrm{H}e_2^2}{\varepsilon_2(\mathrm{H}_2-\mathrm{H}_1)}\{Q_j^*(0)-Q_j^*(1)+(\omega \mathrm{H})^2 CC_j\} \times [Q_m(q_1)-Q_m(q_3)]\right]p_m = \frac{\mathrm{H}e_2}{\mathrm{H}_1-\mathrm{H}_2}\{[Q_j^*(0)-Q_j^*(1)]+(\omega \mathrm{H})^2 CC_j\}U, \quad (13a)$$

where U is an arbitrary value. Substituting the electric displacement obtained from Eq. (11) into Eq. (10b) gives the electric input admittance of the resonator:

$$Y_{\mathrm{in}}=\frac{I}{U}=\frac{i\omega S}{\beta_2(H_1-H_2)}\left(\frac{\mathrm{H}e_2 h_2}{\mathrm{H}_1-\mathrm{H}_2}[Q_m(q_1)-Q_m(q_3)] \times\left[\frac{c_2^D}{\rho_2}(AA1_{jm}+(\omega \mathrm{H})^2 BB1_{jm})+\frac{\mathrm{H}e_2^2}{\varepsilon_2(\mathrm{H}_2-\mathrm{H}_1)} \times\{Q_j^*(0)-Q_j^*(1)+(\omega \mathrm{H})^2 CC_j\}[Q_m(q_1)-Q_m(q_3)]\right]^{-1} \times\{Q_j^*(0)-Q_j^*(1)+(\omega \mathrm{H})^2 CC_j\}-1\right). \quad (13b)$$

To assess the proposed polynomial approach and to highlight its capabilities, our results were compared to the numerical results calculated from the electric input impedance written from Sittig's model:[8]

$$Z_{\mathrm{in}}=\frac{1}{j\omega C_0}\left[1+\frac{k_t^2}{\varphi}\frac{j(z_t+z_b)z_p\sin\varphi-2z_p^2(1-\cos\varphi)}{(z_p^2+z_t z_b)\sin\varphi-j(z_t+z_b)z_p\cos\varphi}\right], \quad (14)$$

where z_t, z_b, and z_p denote the acoustic impedances of the top and bottom electrodes and the piezolayer, respectively. $\varphi=\omega \mathrm{H}/V_p$ (V_p is the thickness mode velocity within the piezolayer) is the electromechanical coupling coefficient.

3. Modal analysis

Modal analysis is a specific case of harmonic analysis obtained by cancellation of the electrical excitation. Under this condition, both the current excitation Equation (12a) and the voltage excitation equation (13a) are reduced to an eigenvalue problem.

In the open-circuit case obtained for $I=0$, the eigenvalues give the antiresonance frequencies

$$(\omega \mathrm{H})^2\delta_{jm}p_m=-BB1_{jm}^{-1}AA1_{jm}p_m, \quad (15a)$$

where δ_{jm} denotes the Kronecker symbol.

Similarly, in the short-circuit case obtained for $U=0$, the eigenvalues give the resonance frequencies

TABLE I. Material parameters used in simulations. Legendre polynomials truncation order is $M=15$.

Parameters	Symbol	ZnO	Aluminum
Density (kg m^{-3})	ρ	5.676	2.7
Elastic stiffness (10^{10} N m^{-2})	c_{33}	21.09	10.7
Elastic viscosity (10^{-3} Pa s)	η	11.96	8.54
Piezoelectric constant (C m^{-2})	e_{33}	1.14	0
Permittivity (10^{-10} F m^{-1})	ε_{33}	0.783	$\approx$0
Layer thickness (μm)	H	2	Modifiable

$$(\omega \mathrm{H})^2\delta_{jm}p_m=-\left[\frac{c_2^D}{\rho_2}BB1_{jm}+\frac{\mathrm{H}e_2^2}{\varepsilon_2(\mathrm{H}_2-\mathrm{H}_1)}CC_j[Q_m(q_1)-Q_m(q_3)]\right]^{-1} \times\left[\frac{c_2^D}{\rho_2}AA1_{jm}+\frac{\mathrm{H}e_2^2}{\varepsilon_2(\mathrm{H}_2-\mathrm{H}_1)}[Q_j^*(0)-Q_j^*(1)] \times[Q_m(q_1)-Q_m(q_3)]\right]p_m. \quad (15b)$$

In both cases, the corresponding eigenvectors p_m yield the field profiles inside the resonator.

The unloaded quality factor Q and the effective electromechanical coupling coefficient k_{eff}^2 are calculated from the resonance and antiresonance frequencies f_r and f_a as follows:[9]

$$Q=\frac{f}{2R_m}\left.\frac{\partial X_m}{\partial f}\right|_{f=f_r}, \quad (16a)$$

$$k_{\mathrm{eff}}^2=\frac{f_a^2-f_r^2}{f_a^2}, \quad (16b)$$

where R_m, X_m, f_r, and f_a represent the motional resistance, the motional reactance, the resonance frequency, and the antiresonance frequency, respectively.

III. NUMERICAL SIMULATIONS

The particle displacement u_2 is expanded in an infinite series of Legendre polynomials. In practice, the infinite summations are truncated to a finite value M when higher-order terms become essentially negligible. Depending on the analysis type, the problem requires a system of $M+1$ linear equations with $M+1$ unknowns for the harmonic analysis or an eigenvalue system with $M+1$ eigenmodes for the modal analysis to be solved. The solutions to be accepted are those for which convergence is obtained as M is increased.[3–6]

A. Material parameters used in simulations

The truncation order and the material constants used in this paper are shown in Table I.

B. Harmonic analysis

We used our method to calculate the electric input admittance of a 2 μm Al/ZnO/2 μm Al BAW resonator with both the classic and anticipation methods and also with an analytical method. The results are shown in Figs. 2(a) and

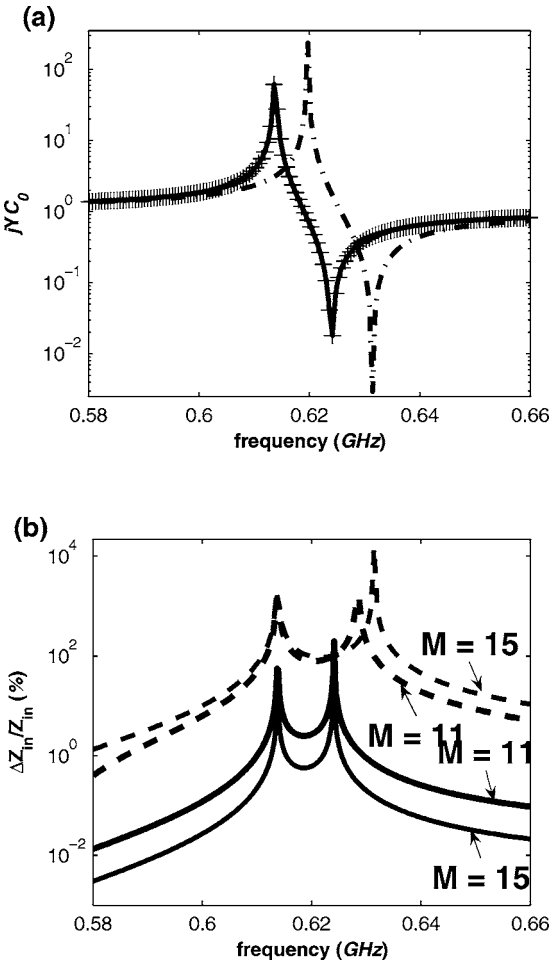

FIG. 2. (a) Comparison of electric input admittance. (b) Effect of truncation order on the convergence of the polynomial methods for the 2 μm Al/ZnO/2 μm Al resonator (solid line: analytical method; broken line: classical method; +: anticipation method).

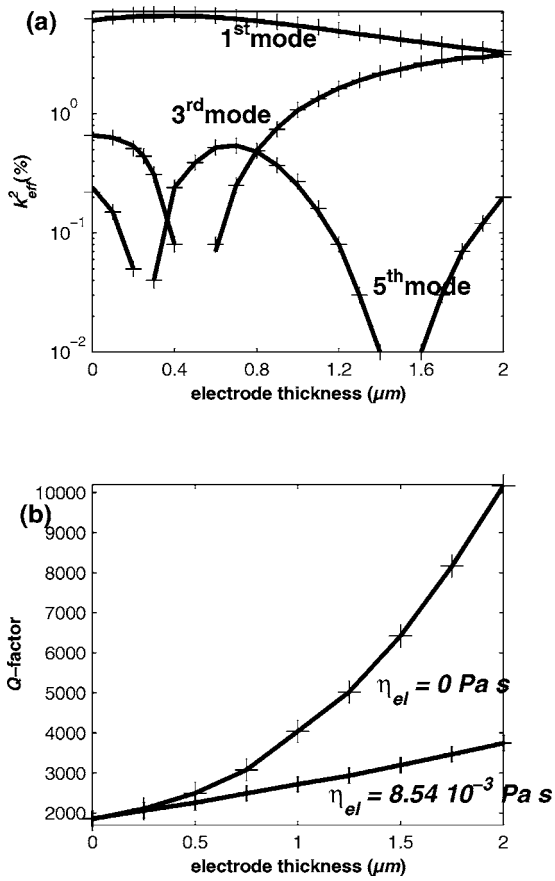

FIG. 3. For a 2 μm ZnO layer and aluminum electrodes: (a) effective electromechanical coupling coefficient; (b) Q factor (solid line: analytical method; +: anticipation polynomial method). $M=15$.

2(b). Figure 2(a) gives the admittance: our results using the anticipation method (+) with a truncation order $M=15$ coincided exactly with the analytically calculated ones (solid line). The results using the classical method did not coincide at all. Figure 2(b) shows the relative error for two different truncation orders, $M=11$ and $M=15$, for both the classical (broken line) and anticipation (solid line) methods. Unlike the anticipation method, higher truncation orders for the classical method result in larger errors rather than higher precision. This is due to badly conditioned matrices with the classical method.

Figure 3 shows the influence of viscosity and electrode thickness on the effective electromechanical coupling coefficient and Q factor. The agreement is quite good between the results calculated using the anticipation method (+) and those calculated analytically (solid line). For the electromechanical coupling coefficient, these curves reveal an optimal electrode thickness for which K^2 is maximum, 0.5 μm for the first mode and 0.7 μm for the fifth mode. For the Q factor, the electrodes and the elastic viscosity of their constituent metal modify the filter performances, as shown in Fig. 3(b). This involves the reduction in the filter bandwidth. With the anticipation polynomial method, the effect of the electrode elastic viscosity can be treated quite simply.

C. Modal analysis

By canceling the sources, the current excitation equation (12a) and the voltage excitation equation (13b) are reduced to eigenvalue equations (15a) and (15b), respectively. In the first case, $I=0$ (open circuited), the eigenvalues yield the antiresonance frequencies; in the second case, $U=0$ (short circuited), the eigenvalues yield the resonance frequencies.

In both cases, the corresponding eigenvectors p_m yield the field profiles within the resonator. Figure 4 shows the effect of electrode thickness on the resonance and antiresonance frequencies for the first five modes. Good agreement between the analytically calculated results and the polynomial anticipation results was obtained.

With the eigenvectors p_m, a closed expression for particle displacement is obtained, and thus other quantities such as electric potential, strain, and electric fields may be determined as well. Figure 5 shows the particle displacement and the stress within the structure. In this figure, once more, good agreement was obtained between the analytical results and the polynomial anticipation results. An important discrepancy was obtained with the classical polynomial method, particularly for the stress, showing divergence in the results due to badly conditioned matrices. All these illustrations validate the polynomial anticipation method for studying BAW resonators.

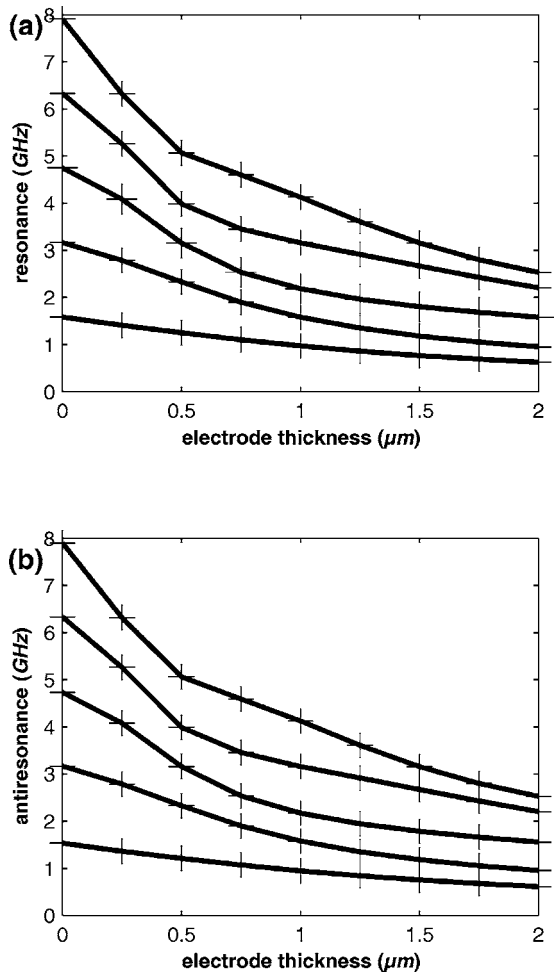

FIG. 4. (a) Resonance frequencies vs electrode thickness. (b) Antiresonance frequencies vs electrode thickness (solid line: analytical results; +: anticipation polynomial method). $M=15$.

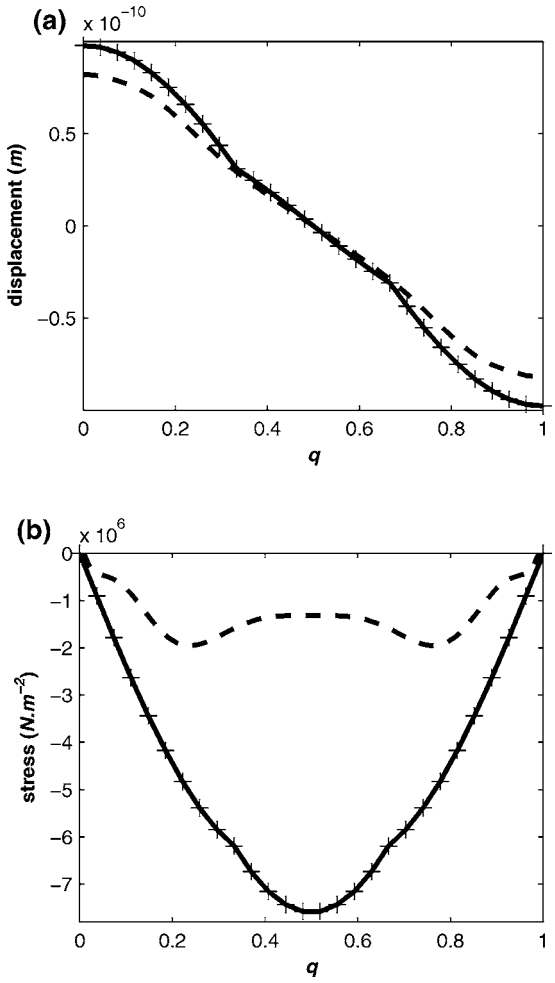

FIG. 5. For a 2 μm ZnO layer and aluminum electrodes at $f_r=0.625$ GHz: (a) particle displacement profiles; (b) stress profiles (solid line: analytical results; broken line: classical method; +: anticipation method). $M=15$.

IV. SUMMARY AND CONCLUSIONS

The Legendre polynomial method has been extended for modeling composite BAW resonators. Incorporation of the stress slope discontinuity directly into the mechanical displacement allows the polynomial method to be used with structures made up of layers of very dissimilar materials. The extension to standing waves and the incorporation of sources, either voltage or current, yield a unique formalism allowing both harmonic and modal analyses. The electric input impedance, the resonance and antiresonance frequencies, the electromechanical coefficient, the quality factor, and the field profiles are easily obtained for an Al/ZnO/Al BAW resonator. The numerical results are in excellent agreement with the analytical results.

The structure was assumed to be laterally unbounded, with no variations in the lateral directions. The technique may be extended to laterally bounded structures by incorporating their geometry directly into the constitutive and propagation equations, as it has been done in this paper for a laterally unbounded resonator. This two-dimensional problem, for which no analytical solution is available, is now being explored.

APPENDIX A: APPROPRIATE MECHANICAL DISPLACEMENTS

The mechanical displacement expressions u_1 and u_3 in the top and bottom electrodes, respectively, need to be determined. Starting from the particle displacement $u_L(q)=p_m Q_m(q)$ in the range $0\leqslant q\leqslant 1$, let us define, for future need, a fictitious stress $T_L(q)=(c_2^D/\mathrm{H})(\partial u_L/\partial q)-h_2 D_0$ also in the range $0\leqslant q\leqslant 1$.

The motion equations in the different layers allow the mechanical displacements on each side of the interfaces to be expressed.

At the interface $q=q_1$, between the top electrode and the piezolayer:

$$u_1(q_1^-)=-\frac{1}{\rho_1 \mathrm{H}\omega^2}\left.\frac{\partial T_1}{\partial q}\right|_{q=q_1^-},$$

$$u_2(q_1^+)=-\frac{1}{\rho_2 \mathrm{H}\omega^2}\left.\frac{\partial T_2}{\partial q}\right|_{q=q_1^+}.$$

Similarly, at the interface $q=q_3$ between the piezolayer and the bottom electrode:

$$u_2(q_3^-) = -\frac{1}{\rho_2 \mathrm{H}\omega^2} \left.\frac{\partial T_2}{\partial q}\right|_{q=q_3^-}.$$

$$u_3(q_3^+) = -\frac{1}{\rho_3 \mathrm{H}\omega^2} \left.\frac{\partial T_3}{\partial q}\right|_{q=q_3^+}.$$

Given the continuity of the particle displacements through the interfaces, it can be written as

$$\frac{1}{\rho_1} \left.\frac{\partial T_1}{\partial q}\right|_{q=q_1^-} = \frac{1}{\rho_2} \left.\frac{\partial T_2}{\partial q}\right|_{q=q_1^+} = \frac{1}{\rho_2} \left.\frac{\partial T_L}{\partial q}\right|_{q=q_1^+},$$

$$\frac{1}{\rho_3} \left.\frac{\partial T_3}{\partial q}\right|_{q=q_3^+} = \frac{1}{\rho_2} \left.\frac{\partial T_2}{\partial q}\right|_{q=q_3^-} = \frac{1}{\rho_2} \left.\frac{\partial T_L}{\partial q}\right|_{q=q_3^-}.$$

In order (i) to anticipate the stress slope discontinuity at the interface and (ii) to fulfill the requirements of stress continuity at the interface, these relations allow the stress in each electrode to be written as

$$T_1(q) = \frac{\rho_1}{\rho_2} T_L(q) + \left(1 - \frac{\rho_1}{\rho_2}\right) T_L(q_1),$$

$$T_3(q) = \frac{\rho_3}{\rho_2} T_L(q) + \left(1 - \frac{\rho_3}{\rho_2}\right) T_L(q_3).$$

Using Hooke's law in the electrodes, it is easy to calculate the mechanical displacements u_1 and u_3:

$$u_i(q) = \frac{\rho_i}{\rho_2}\frac{c_2^D}{c_i} u_L(q) + \frac{c_2^D}{c_i}\left(1 - \frac{\rho_i}{\rho_2}\right)(q - q_i) \left.\frac{\partial u_L}{\partial q}\right|_{q=q_i} + \left(1 - \frac{\rho_i}{\rho_2}\frac{c_2^D}{c_i}\right) u_L(q_i) - \frac{\mathrm{H}h_2}{c_i}(q - q_i) D_0, \quad i = 1,3,$$

where $q_1 = \mathrm{H}_1/\mathrm{H}$ and $q_3 = \mathrm{H}_2/\mathrm{H}$.

APPENDIX B: MATRICES OF THE INFINITE SYSTEM OF LINEAR EQUATIONS

$$AA1_{jm} = \rho_1\left(b_{jm}^{0,q_1} - \left.\frac{\partial Q_m}{\partial q}\right|_{q=q_1} c_{j0}^{0,q_1}\right) + \rho_2\left(b_{jm}^{q_1,q_3} + \left.\frac{\partial Q_m}{\partial q}\right|_{q=q_1} c_{j0}^{0,q_1} + \left.\frac{\partial Q_m}{\partial q}\right|_{q=q_3} c_{j0}^{q_3,1}\right) + \rho_3\left(b_{jm}^{q_3,1} - \left.\frac{\partial Q_m}{\partial q}\right|_{q=q_3} c_{j0}^{q_3,1}\right).$$

$$BB1_{jm} = \frac{\rho_1^2}{c_1}\left(a_{jm}^{0,q_1} - \left.\frac{\partial Q_m}{\partial q}\right|_{q=q_1} d_{j0}^{0,q_1,q_1} - Q_m(q_1) a_{j0}^{0,q_1}\right) + \frac{\rho_2^2}{c_2^D} a_{jm}^{q_1,q_3} + \frac{\rho_3^2}{c_3}\left(a_{jm}^{q_3,1} - \left.\frac{\partial Q_m}{\partial q}\right|_{q=q_3} d_{j0}^{q_3,1,q_3} - Q_m(q_3) a_{j0}^{q_3,1}\right) + \frac{c_2^D}{\rho_2}(\rho_1 Q_m(q_1) a_{j0}^{0,q_1} + \rho_3 Q_m(q_3) a_{j0}^{q_3,1}) + \rho_2\left(\frac{\rho_1}{c_1} \cdot \left.\frac{\partial Q_m}{\partial q}\right|_{q=q_1} d_{j0}^{0,q_1,q_1} + \frac{\rho_3}{c_3} \left.\frac{\partial Q_m}{\partial q}\right|_{q=q_3} d_{j0}^{q_3,1,q_3}\right),$$

$$CC_{\mathrm{j}} = e_2\left[\frac{\rho_1}{c_1} d_{j0}^{0,q_1,q_1} + \frac{\rho_3}{c_3} d_{j0}^{q_3,1,q_3}\right],$$

with

$$q_1 = \frac{\mathrm{H}_1}{\mathrm{H}}, \quad q_3 = \frac{\mathrm{H}_2}{\mathrm{H}},$$

$$a_{jm}^{\alpha,\beta} = \int_0^1 Q_j^*(q)\pi_{\alpha,\beta}(q) Q_m(q) dq = \frac{\sqrt{(2j+1)(2m+1)}}{2}\frac{(2j)!}{2^{\mathrm{j}}(j!)^2}\frac{(2m)!}{2^m(m!)^2} \times \left[\frac{\chi_j \chi_m}{j+m+1} z^{j+m+1} + \frac{\chi_{j-2}\chi_m + \chi_j \chi_{m-2}}{j+m-1} z^{j+m-1} + \cdots\right]_{2\alpha-1}^{2\beta-1},$$

where

$$\chi_{j-n} = (-1)^{n/2}\frac{j(j-1)(j-2)\cdots(j-n+1)}{2.4\cdots n(2j-1)(2j-3)\cdots[2j-(n-1)]},$$

$$b_{jm}^{\alpha,\beta} = \int_0^1 Q_j^*(q)\frac{\partial}{\partial q}\left[\pi_{\alpha,\beta}(q)\frac{\partial Q_m}{\partial q}\right] dq = c_{jm}^{\alpha,\beta} + 2\sqrt{2m+1}[\sqrt{2m-1}\, e_{jm-1}^{\alpha,\beta} + \sqrt{2m-5}\, e_{jm-3}^{\alpha,\beta} + \sqrt{2m-9}\, e_{jm-5}^{\alpha,\beta} + \cdots],$$

$$c_{jm}^{\alpha,\beta} = Q_j^*(\alpha)Q_m(\alpha) - Q_j^*(\beta)Q_m(\beta) = \sqrt{(2j+1)(2m+1)}[P_j^*(2\alpha-1)P_m(2\alpha-1) - P_j^*(2\beta-1)P_m(2\beta-1)],$$

$$d_{jm}^{\alpha,\beta,\gamma} = \int_0^1 Q_j^*(q)\pi_{\alpha,\beta}(q)(q-\gamma)Q_m(q) dq = \left(\frac{1}{2} - \gamma\right) a_{jm}^{\alpha,\beta} + \frac{1}{2}[f(m+1)a_{jm+1}^{\alpha,\beta} + f(m)a_{jm-1}^{\alpha,\beta}],$$

with

$$e_{jm}^{\alpha,\beta} = \int_0^1 Q_j^*(q)\frac{\partial}{\partial q}[\pi_{\alpha,\beta}(q)Q_m(q)] dq = 2\sqrt{2m+1}[\sqrt{2m-1}\, a_{jm-1}^{\alpha,\beta} + \sqrt{2m-5}\, a_{jm-3}^{\alpha,\beta} + \sqrt{2m-9}\, a_{jm-5}^{\alpha,\beta} + \cdots],$$

$$f(m) = \frac{m}{\sqrt{(2m-1)(2m+1)}}.$$

[1] T. Nishihara, T. Yokoyama, T. Miyashita, and Y. Satoh, 2002 IEEE International Ultrasonics Symposium, 2002 (unpublished), Vol. 1, p. 969.

[2]S. Mahon and R. Aigner, CS Mantech Conference, 2007 (unpublished), p. 15.
[3]S. Datta and B. J. Hunsinger, J. Appl. Phys. **49**, 475 (1978).
[4]Y. Kim and W. D. Hunt, J. Appl. Phys. **68**, 4993 (1990).
[5]J. E. Lefebvre, V. Zhang, J. Gazalet, and T. Gryba, J. Appl. Phys. **83**, 28 (1998).
[6]L. Elmaimouni, J. E. Lefebvre, V. Zhang, J. Gazalet, and T. Gryba, Wave Motion **42**, 177 (2005).
[7]D. Royer and E. Dieulesaint, *Elastic Wave in Solids I* (Springer, Berlin, 2000).
[8]E. K. Sittig, *Physical Acoustics* (Academic, New York, 1972), Vol. 9, Chap. 5.
[9]J. F. Rosenbaum, *Bulk Acoustic Wave Theory and Devices* (Artech, Boston, 1988).